High Performance No-Flow Underfills for Low-Cost Flip-Chip Applications: Material Characterization

C. P. Wong, *Fellow, IEEE,* Songhua H. Shi, and G. Jefferson

***Abstract*—Underfill encapsulant is critical to the reliability of the flip-chip solder joint interconnects. Novel no-flow underfill encapsulant is an attractive flip-chip encapsulant due to the simplification of the no-flow underfilling process. To develop the no-flow underfill material suitable for the no-flow underfilling process of flip-chip solder joint interconnects, we have studied and developed a series of metal chelate latent catalysts for the no-flow underfill formulation. The latent catalyst has minimal reaction with the epoxy resin (cycloaliphatic type epoxy) and the crosslinker (or hardener) at the low temperature ($< 180\ ^{\circ}$C) prior to the solder reflow and then rapid reaction takes place to form the low-cost high performance underfills. The effects of the concentration of the hardener and catalyst on the curing profile and physical properties of the cured formulations were studied. The kinetics and exothermic heat of the curing reactions of these formulations were investigated by differential scanning calorimetry (DSC). Glass transition temperature (T_g) and thermal coefficient of expansion (TCE) of these cured resins were investigated by thermo-mechanical analyzer (TMA). Storage moduli (E', E'') and crosslinking density of the cured formulations were measured by dynamic-mechanical analyzer (DMA). Weight loss of these formulations during curing was investigated by thermo-gravimetric analyzer (TGA). Additionally, some comparison results of our successful novel generic underfills with the current commercial experimental no-flow underfills are reported.**

***Index Terms*—Catalyst, epoxy and anhydride, flip-chip, metal chelate, no-flow underfill.**

I. Introduction

POLYMERIC materials are increasingly being used in microelectronics applications because of their low cost and high performance properties such as low dielectric constant, ease in process, etc. [1]. An important trend of developing a semiconductor device is the miniaturization, aiming at high density and complex functionality of electronic products. Accompanying this trend, controlled collapse chip connection (C^4) and direct chip attachment (DCA) technology are attracting attentions and developments [2]. While C^4 and DCA techniques become popular, the problem with TCE mismatch between the silicon IC chip and the high TCE and low-cost organic substrate becomes critical, in particular with the larger IC chips and fine-pitch, low profile solder joints. Due to the thermal mismatch between the silicon IC (2.5 ppm) and low cost organic substrates, in particularly, the FR-4 printed wiring board (18–24 ppm/°C), the temperature cycling excursions generate tremendous thermo-mechanical stress to the solder joints and subsequently result in performance degradation of packaged systems. The underfill serves as an adhesive to reinforce the physical and mechanical properties of the solder joints between the chip and the substrate. The encapsulant does not only provide drastic fatigue life enhancement, but also provides the corrosion protection of the IC, resulting in ten to hundred folds improvement in fatigue life as compared to an unencapsulated package [3]. As such, the new technique of underfill encapsulation has been gaining acceptance [4].

However, most of current underfill encapsulants are dispensed on one or two edges of an assembled flip-chip package. This allows capillary action to draw the underfill into the gap between the chip and substrate of the assembled package to complete the encapsulation process as shown in Fig. 1. Some of the state-of-the-art underfill encapsulants can completely fill a ~2 mil (~50 μm) gap with 1/4 in (6.35 mm) chip within one minute. But the process of reflowing solder bump and the process of underfilling and curing the encapsulants are separate processing steps, as such, it results in lower production efficiency.

The No-flow underfilling process was invented to simultaneously reflow solder bump and cure the underfill [4]–[6], [10]–[11]. As shown in Fig. 2. The No-flow underfilling process not only eliminates the strict limits on the viscosity of underfill encapsulants and package size, but also improves the production efficiency.

A successful no-flow underfill encapsulant should meet the following requirements.

1) Minimal curing reaction occurs at the temperature below solder bump reflow temperature (~180–210 °C).
2) Rapid curing reaction takes place after the completion of the solder bump reflow.
3) Good adhesion to the passivation layer of chips, substrates, solder masks and solder joints.
4) Low TCE and reasonable moduli to minimize the residual thermal stress resulted from the curing process and subsequent cooling.

Based on these requirements, epoxy-based encapsulant was chosen for the no-flow underfill material. Some advantages of epoxy resins are low-cost, adjustable curing temperature and curing rate (by selecting proper catalyst), good adhesion to most of substrates. However, little research work was done in

Manuscript received February 1, 1998; revised May 1, 1998. This work was supported by NSF, The Georgia Tech Packaging Research Center, and DARPA. This paper was recommended for publication by Associate Editor C. C. Lee upon evaluation of the reviewers' comments.

The authors are with the School of Materials Science and Engineering and Packaging Research Center, Georgia Institute of Technology, Atlanta, GA 30332-0245 USA (e-mail: cp.wong@mse.gatech.edu).

Publisher Item Identifier S 1070-9886(98)05901-0.

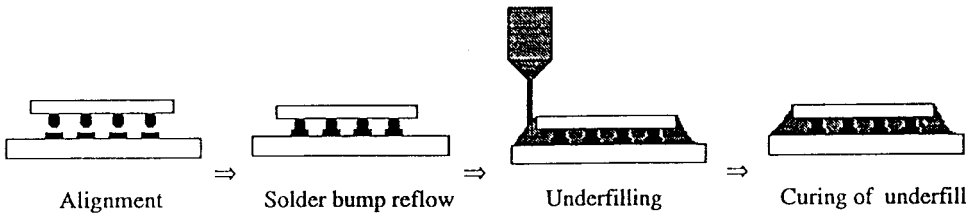

Fig. 1. Conventional underfilling process.

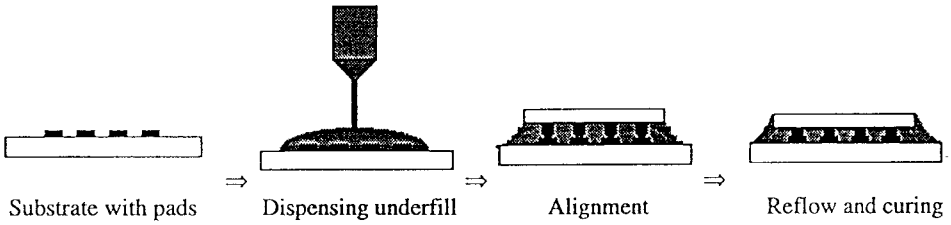

Fig. 2. No-flow underfilling process.

TABLE I
INGREDIENTS OF NO-FLOW UNDERFILL FORMULATION

Name of Chemicals	Structure of Chemicals	Usage Quantity (parts by weight)
Cycloaliphatic Epoxy Resin	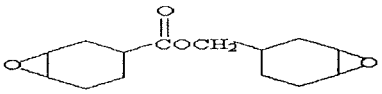	100
Curing Hardener	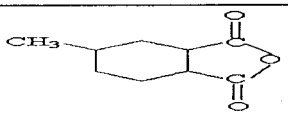	30~100
Curing Catalysts	$[CH_3COCH=C(O^-)CH_3]_2Co^{2+}$	0.1~1

this area and few successful commercial products are available. Therefore, this paper explored some potential epoxy-based formulations for the no-flow underfill application, characterized their properties and studied their reaction mechanism.

II. EXPERIMENTS

A. Chemical Ingredients of the No-Flow Underfill Material

Table I lists the chemical structures of epoxy resin, hardener and catalysts used in the experiments. The epoxy resin is 3, 4-epoxy cyclohexyl methyl-3, 4-epoxy cyclohexyl carboxylate provided by Union Carbide under the trade name ERL-4221D and used as received. The molecular weight and epoxide equivalent weight (EEW) of the epoxy resin is 252.3 g/mol and 133 g, respectively. The hardener (or crosslinker) is hexahydro-4-methylphthalic anhydride (HMPA) purchased from Aldrich Chemical Company, Inc. and used as received. HMPA molecular weight is 168.2 g/mol and its purity is more than 97%. Co(II) acetylacetonate was used as curing catalyst for this study. Their usage quantities are listed in Table I.

B. Preparation of Underfill Formulations

The specified quantity of hardener was added into the epoxy resin and the mixture was stirred for 15 min at 60–70 °C. Thereafter, a specified quantity of catalyst was added into the mixture and stirred for additional 30 minutes at 60–70 °C until the catalyst was homogeneously dissolved. The formulations were then stored in a freezer at −40 °C. When fillers or other additives are incorporated in these formulations, the frozen formulations would be warmed to room temperature and the desired fillers or additives could be incorporated into the master batch formulations.

C. Measurement Methods

1) Curing Profile and Differential ScanningCalorimetry (DSC) Measured Glass Transition Temperature T_g^{DSC}: To study the curing profile and T_g of our underfill formulations, a modulated DSC instrument (by TA Instruments, Model 2920) was used. A sample of ∼10 mg of an underfill which had been equilibrated to room temperature from −40 °C, was placed into a hermetic DSC sample pan. The sample was then heated in the DSC cell at 5 °C/min to around 300 °C to obtain the curing profile. To obtain the T_g^{DSC} of the sample, the cured sample was left in the DSC cell and was cooled down to room temperature at 5 °C/min. Then the sample was reheated to 280 °C at 5 °C/min to obtain the T_g^{DSC} of the cured sample.

2) Thermal Coefficient of Expansion (TCE) and Thermo-Mechanical Analyzer (TMA) Measured Glass

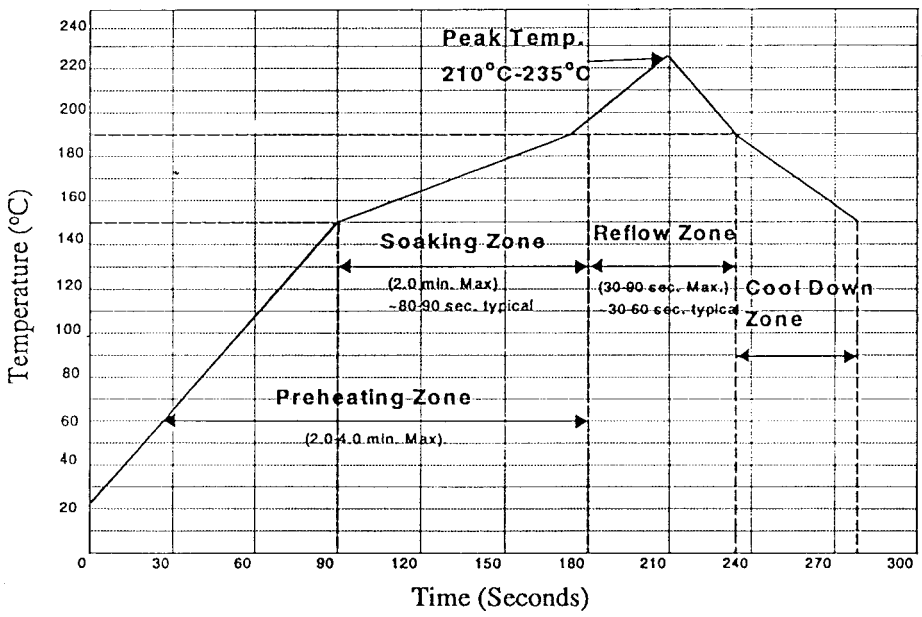

Fig. 3. Typical heating profile of eutectic tin/lead solder bumps.

Transition Temperature T_g^{TMA}*:* Measurement of TCE and T_g^{TMA} of a cured formulation was performed on a TMA instrument (by TA Instruments, Model 2940). A specimen for TMA testing was made by placing a liquid formulation into an aluminum pan (1.5-in diameter), then the specimen was transferred to a 80 °C preheated convective oven, and then heated to 250 °C at 3 °C/min. Then, the sample was isothermally cured in the 250 °C oven for another 15 min. After this heating, the sample was then removed from the oven and cooled to room temperature. A diamond saw was used to cut the cured sample into strips with dimensions of about 5 × 5 × 2 mm. After placing a specimen in the TMA instrument, heat was applied from room temperature to about 250 °C at a rate of 5 °C/min. The thermal coefficient of linear expansion was obtained from the thermal expansion quantity versus temperature. The inflection point of thermal expansion was defined as T_g^{TMA}.

3) Dynamic Moduli and Dynamic Mechanical Analyzer (DMA) Measured Glass Transition Temperature T_g^{DMA}*:* The preparation of a specimen used for the DMA testing was the same as for the TMA testing and the experiments were performed on a DMA instrument (by TA Instruments, Model 2980). However, the dimension of the specimens for DMA test is longer and wider, about 32 × 11 × 3 mm. The measurement was performed in single cantilever mode under 1 Hz sinusoidal strain loading. Storage moduli (E'), loss moduli (E''), and loss tangent $(\tan\delta)$ were calculated by the preinstalled software. The peak temperature of $\tan\delta$ was defined as the T_g^{DMA}.

4) Thermo-Gravimetric Analyzer Measured Weight Loss: The weight loss of the formulations during curing was studied by a TGA instrument (by TA Instruments, Model 2050). A sample of ∼40 mg of a liquid formulation which had been equilibrated to room temperature from −40 °C, was placed into a platinum TGA sample pan. The sample was then heated in the TGA furnace at 10 °C/min to about 280 °C under N_2 purging (N_2 flow rate: 77 ml/min in vertical direction and 12 ml/min in horizontal direction). The percentage of weight difference between 25 °C and 270 °C was taken as the weight loss percentage of the formulation during curing.

III. Results and Discussions

A. Comparison of Curing Profile of Underfills and Heating Profile of Solder Bump Reflow

The basic requirement of a no-flow underfill material must match the reflow profile of a specified solder bump, that is, a minimal curing reaction occurs before solder bump reflow but rapid curing reaction takes place thereafter. Fig. 3 describes the typical heating profile of a low-temperature reflowable eutectic tin/lead solder bump. It is seen that the reflowing peak temperature is higher than the melting point of eutectic solder (∼187 °C). Usually, the reflowing peak temperature goes beyond the melting point of the solder bump materials by 20–40 °C to ensure the completion of wetting of solder melt to metallic pads on the substrate. Accordingly, the no-flow underfill materials should not gel before solder bump reflow but must complete the curing within a couple of minutes after that. Fig. 4 shows the curing profile of several underfill materials, including two commercial samples A and B. Except commercial A, all no-flow underfill formulations fit the heating profile of the eutectic tin/lead solder bump. Since some of our formulations have higher curing peak temperature, they can be used for some other solder bump alloys with higher reflowing temperature. Fig. 5 shows the T_g^{DSC} of these no-flow underfill formulations. Again, except for the commercial A whose T_g is around 93.6 °C, all other formulations have T_g higher than 150 °C, which are suitable for underfill applications. Moreover, most of our no-flow underfill materials show much

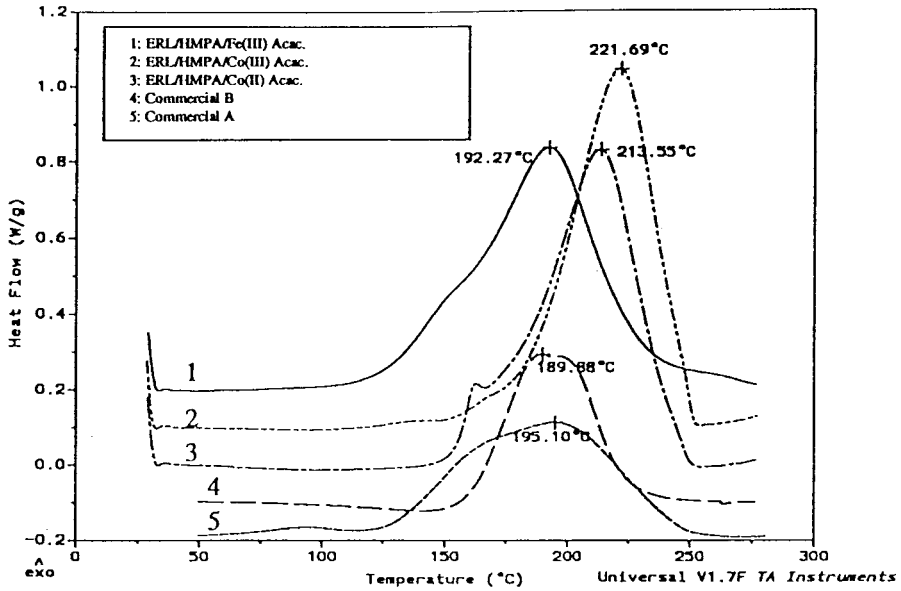

Fig. 4. Curing profile of some no-flow underfills.

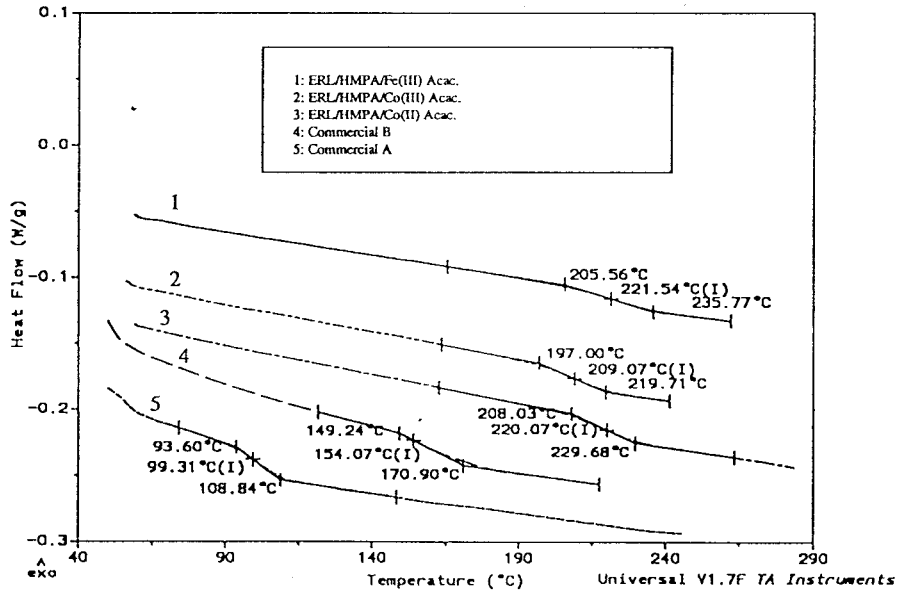

Fig. 5. T_g^{DSC} of the no-flow underfills.

higher T_g's (200 °C and more), which can be explored for higher melting point solder metallurgy.

B. Effects of Hardener Concentration

Fig. 6 shows the relationship between the curing peak temperature and the concentration of the hardener. The concentration of hardener has little effect on the curing peak temperature of the underfills. However, increasing the concentration of hardener can significantly decrease the TCE of the cured formulations in the lower hardener concentration region (<70 wt% of the epoxy resin) and then level off in the higher hardener concentration region, as shown in Fig. 7. The effect

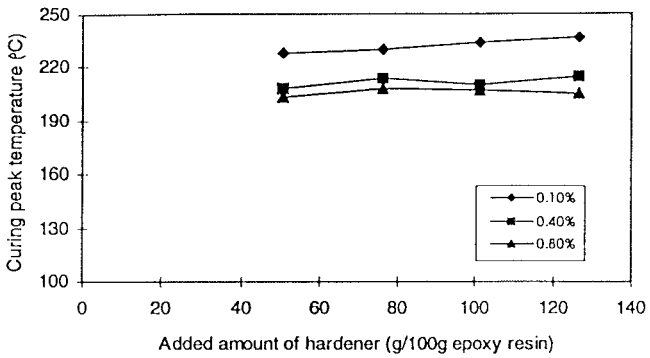

Fig. 6. Effect of hardener concentration on the curing peak temperature.

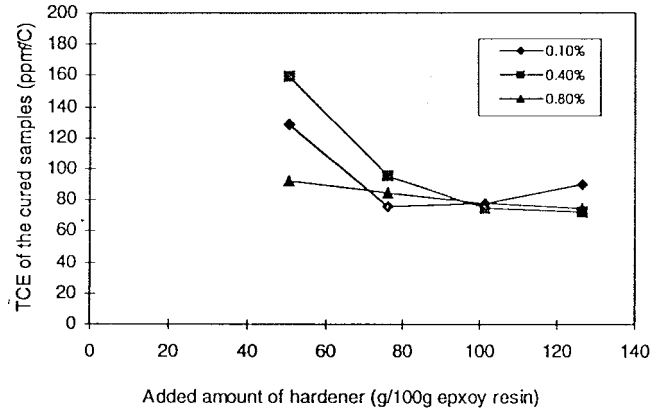

Fig. 7. Effect of hardener concentration on TCE of the cured samples.

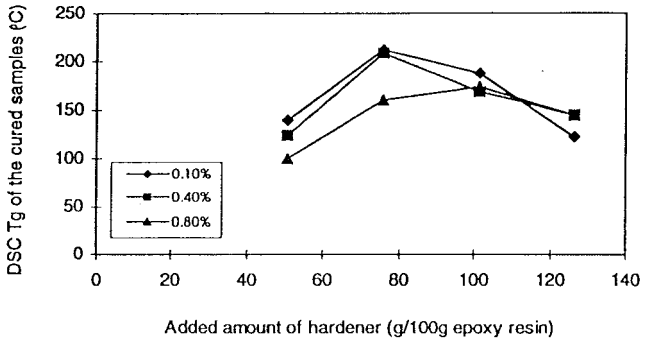

Fig. 8. Effect of hardener concentration on T_g^{DSC} of the cured samples.

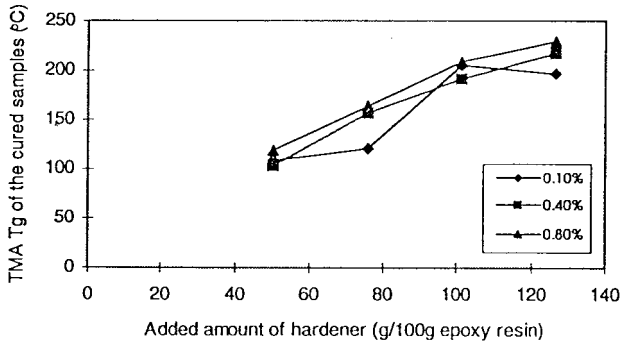

Fig. 9. Effect of hardener concentration on T_g^{TMA} of the cured samples.

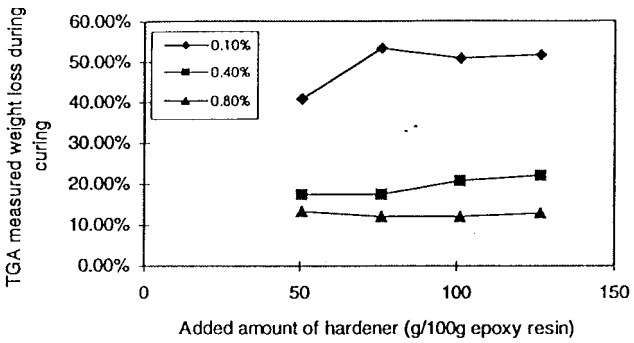

Fig. 10. Effect of hardener concentration on the weight loss of the samples during curing.

of the concentration of hardener on T_g of the cured samples is somehow complex. The measured T_g of the cured samples is different using different measuring methods. Fig. 8 plots the T_g^{DSC} versus the concentration of hardener. It shows that there is a hardener concentration ($\sim$80 wt% of epoxy resin) at which the T_g^{DSC} of the cured formulation has a highest value. In the region lower than this hardener concentration, increasing the concentration of the hardener can greatly increase the T_g^{DSC} of the cured samples; whereas in the region higher than this concentration, increasing the hardener concentration only results in the decrease of T_g^{DSC}. However, T_g^{TMA} of the cured samples increases with increasing the concentration of the hardener within the whole tested concentration range, which is shown in Fig. 9. Fig. 10 is the TGA measured weight loss of the formulations during curing. It indicates that the effect of the hardener concentration on the weight loss depends on the added catalyst level. For low catalyst level (such as 0.1 wt% of the mixture of the epoxy resin and the hardener), the weight loss increases with the increase in the hardener concentration at the low hardener concentration region ($<$80 wt% of the epoxy resin) and level off thereafter. For high catalyst level (such as $>$ 0.4 wt% of the mixture of the epoxy resin and the hardener), the hardener does not show noticeable effect on the weight loss. The various dynamic mechanical properties of the cured samples are tabulated in Table II. Fig. 11 shows the relationship between the T_g^{DMA} and the concentration of the hardener. There is a hardener concentration ($\sim$100 wt% of the epoxy resin) corresponding to the highest T_g^{DMA}. Below this hardener concentration, the T_g^{DMA} significantly increase with increasing the concentration of hardener; whereas above this hardener concentration, the T_g^{DMA} slightly decreases with further increasing the hardener concentration. The case recorded in Fig. 11 is similar to the case described in Fig. 8, except that the highest T_g value appears at higher hardener concentration in Fig. 11 than that in Fig. 8. The last column in Table II is the calculated crosslinking density using kinetic theory of rubber elasticity [9]. The crosslinking density $\rho_{(E')}$ can be determined by (1) as follows:

$$\rho_{(E')} = E'/3\phi RT \tag{1}$$

where E' is the storage elastic modulus of the cured samples at peak temperature of $\tan\delta$+ 40 °C, $\phi = 1$ is a front factor (assumed as $\phi = 1$), R is the gas constant, and T is the absolute temperature. The assumption behind this calculation is that the cured epoxy resin is in real rubbery state at the temperature T_g^{DMA}+ 40 °C. Fig. 12 shows the calculated $\rho_{(E')}$ versus hardener concentration. It shows that the crosslinking density of the cured samples increases with increasing the hardener concentration within the investigated concentration range.

Based on the experimental results mentioned above, the hardener concentration may play dual roles in affecting the final properties of the cured formulations: hardener and plasticizer. On one hand, increasing the hardener concentration in the epoxy resin from 50.58 wt% to 126.46 wt% drives the added amount of anhydride more and more close to its stoichiometric quantity with epoxy resins. Thus the crosslinking

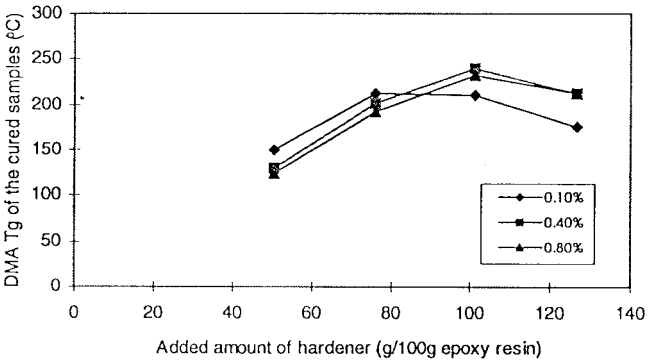

Fig. 11. Effect of hardener concentration on T_g^{DMA} of the cured samples.

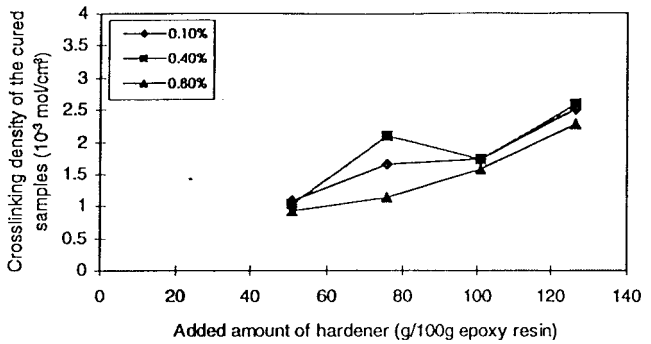

Fig. 12. Effect of hardener concentration on crosslinking density.

density increases with increasing the hardener concentration. Consequently, the TCE and T_g^{TMA} of the cured samples increase with increasing hardener concentration since the TCE and T_g^{TMA} are mainly affected by the crosslinking density. On the other hand, not all the anhydride molecules can effectively react with the epoxy resin and then become the polymeric network. Instead, increasing the concentration of the hardener can increase the concentration of small hardener molecules and/or chain ends in the cured network. These small hardener molecules and chain ends can act as a plasticizer to decrease the T_g^{DSC} and T_g^{DMA} since the free volume of the cured underfill increases with these increasing species. Thus, the net effect of the hardener concentration on T_g^{DSC} and T_g^{DMA} is determined by the competition between the effect from increasing crosslinking density and the effect from increasing small molecule quantity due to the increase of the hardener concentration. Therefore, it is not surprising that there is a hardener concentration corresponding to highest T_g^{DSC} and T_g^{DMA}. Fig. 13 shows the weight loss of the pure epoxy resin and hardener used in all the formulations. It indicates that the hardener begins to vaporize at 100 °C and totally consumes at 220 °C. The epoxy resin begins to vaporize at a higher temperature, and substantially faster at the temperature higher than 200 °C. Thus, the low curing rate at low catalyst level allows more hardener molecules to vaporize at an elevated temperature. At high catalyst level, more volatile molecules (both epoxy resin and hardener) can react and form nonvolatile species during heating due to the higher curing rate, suppressing the hardener concentration effect.

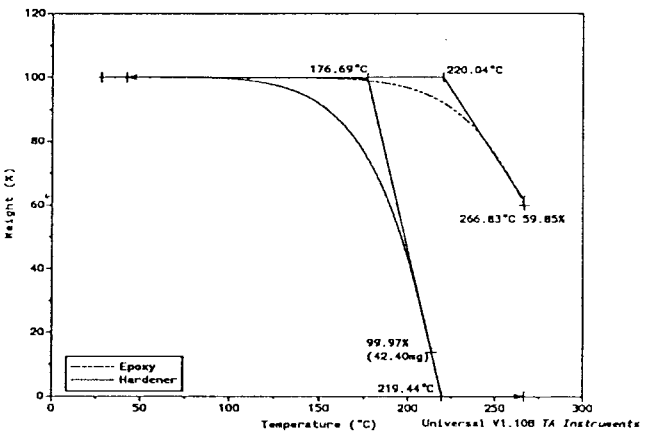

Fig. 13. Weight loss of the neat epoxy resin and neat hardener during heating.

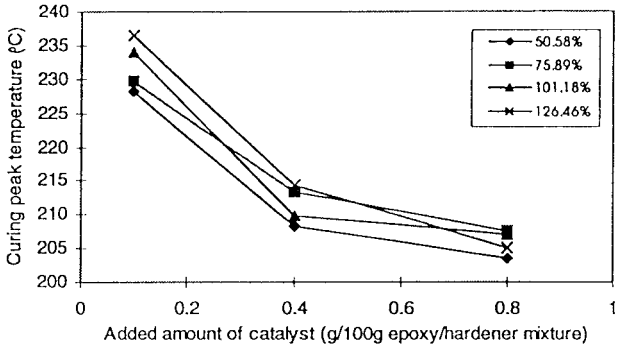

Fig. 14. Effect of catalyst concentration on curing peak temperature.

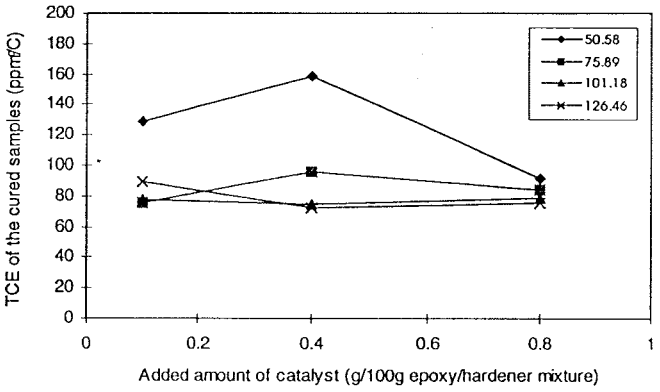

Fig. 15. Effect of catalyst concentration on TCE of the cured samples.

C. Effects of Concentration of Catalyst

Fig. 14 shows that increasing the concentration of catalyst significantly decreases the curing peak temperature. This effect appears more obvious in the low catalyst concentration region. However, increasing the catalyst concentration does not show noticeable effects on the TCE, T_g^{DSC}, T_g^{TMA}, T_g^{DMA} and crosslinking density, which are plotted in Figs. 15–19, respectively. Fig. 20 shows that higher catalyst level always results in lower weight loss of the underfill during curing.

TABLE II
DYNAMIC VISCOELASTIC PROPERTIES AND CROSSLINKING DENSITIES OF THE CURED FORMULATIONS

$C_{catalyst}$[c]	$C_{hardener}$[d]	Tanδ Peak		E'(MPa)[a]			ρ(E')[b] (10^{-3} mol/cm^3)
		Value	Temp (°C)	30 °C	Tg - 60 (°C)	Tg + 40 (°C)	
0.1	50.58	0.665	149.3	3146	2119	12.48	1.08
0.1	75.89	0.494	211.4	2434	1645	21.51	1.64
0.1	101.18	0.519	210.7	2428	1620	22.63	1.73
0.1	126.46	0.461	175.8	2565	1650	30.46	2.50
0.4	50.58	0.815	129.2	2145	1860	11.38	1.03
0.4	75.89	0.546	201.3	2514	1723	26.69	2.08
0.4	101.18	0.557	240.2	2594	1587	24.07	1.74
0.4	126.46	0.460	212.7	2677	1548	33.69	2.57
0.8	50.58	0.878	124.4	2801	2142	10.01	0.92
0.8	75.89	0.719	191.3	2598	1775	14.24	1.13
0.8	101.18	0.542	232.8	2315	1537	21.51	1.58
0.8	126.46	0.560	211.4	2733	1572	29.70	2.27

[a] E' = storage elastic modulus
[b] ρ(E') = crosslinking density
[c] catalyst concentration (g/100g epoxy/hardener mixture)
[d] hardener concentration (g/100g epoxy resin)

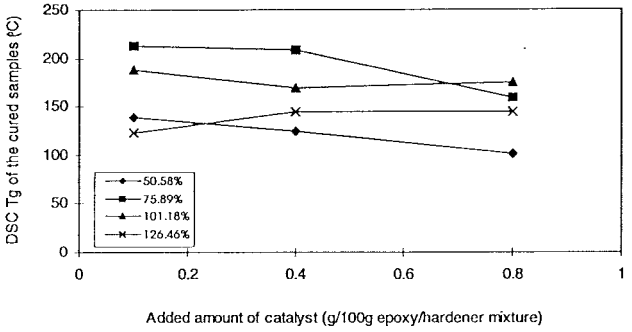

Fig. 16. Effect of catalyst concentration on T_g^{DSC} of the cured samples.

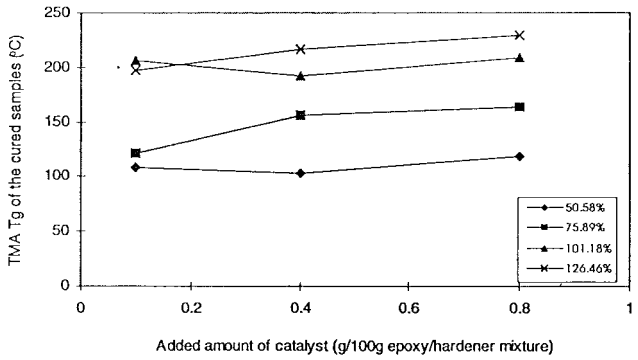

Fig. 17. Effect of catalyst concentration on T_g^{TMA} of the cured samples.

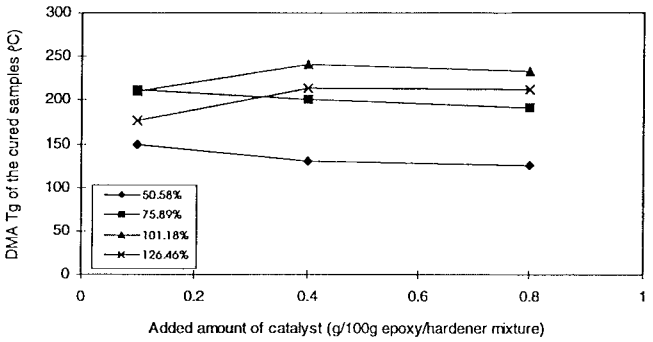

Fig. 18. Effect of catalyst concentration on the T_g^{DMA} of the cured samples.

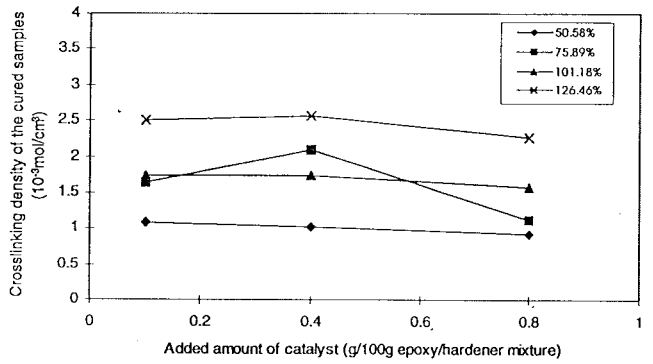

Fig. 19. Effect of catalyst concentration on crosslinking density of the cured samples.

The experimental results above are reasonable. The catalyst, i.e., metal acetylacetonate, generally react with anhydride first to form active species which open the epoxy ring, since metal acetylacetonate or anhydride itself can not effectively open cycloaliphatic epoxy ring even if the temperature goes to 210 °C as shown in Fig. 21. Considering the fact that the added amount of the hardener is much more than the added amount of the catalyst, so increasing the catalyst concentration will increase the concentration of active species, and consequently decrease the curing peak temperature. However, the concentration of active species does not affect the crosslinking density of the cured samples. Due to its very low concentration, the plasticizer effect of catalyst is minimal as compared to the hardener. Therefore, the catalyst concentration does not show any noticeable effect on the final properties of the cured samples. As mentioned above, higher catalyst level always results in higher curing rate, which is translated into the lower weight loss of the underfill during heating.

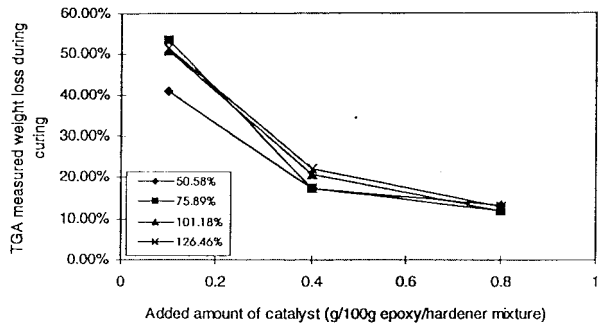

Fig. 20. Effect of catalyst concentration on the weight loss of the samples during curing.

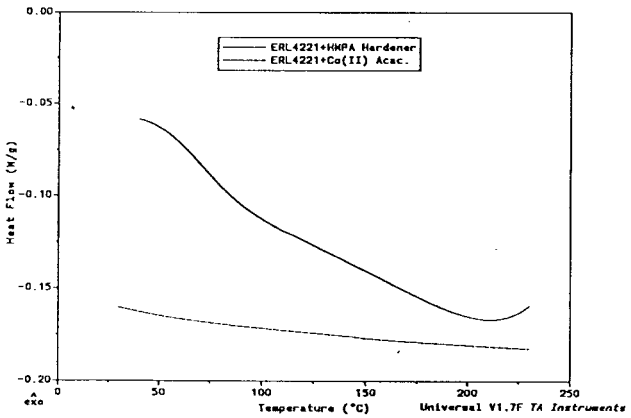

Fig. 21. DSC study indicates that ERL-4221 neither reacts with the HMPA hardener nor reacts with the cobaltous acetylacetonate latent catalyst at the temperaturebelow 200 °C.

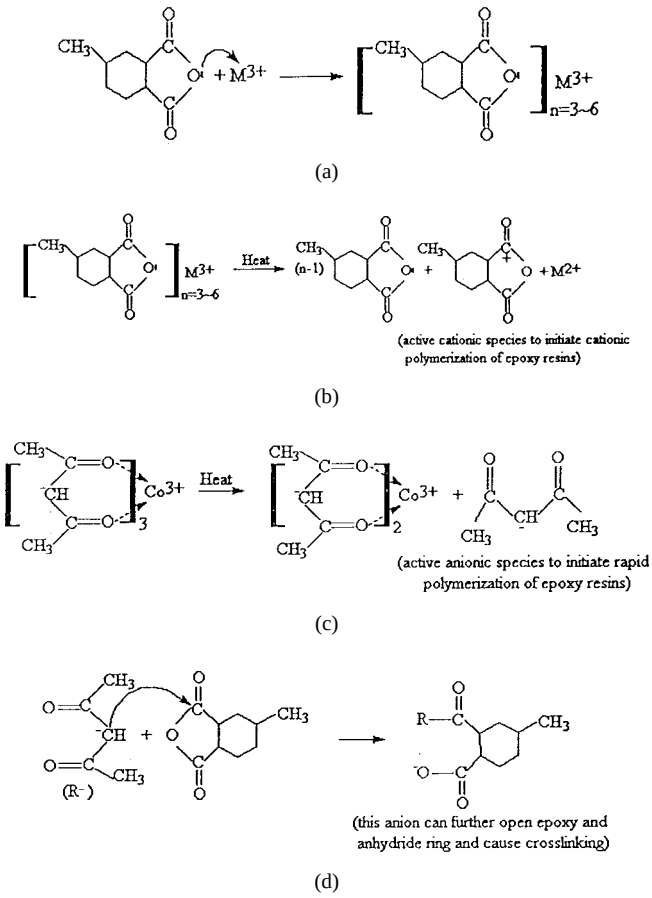

Fig. 22. Possible curing mechanism for epoxy/anhydride/metal acetylacetonate system.

D. Curing Mechanism of Epoxy/Anhydride/Metal Acetylacetonate System

The curing mechanism of epoxy/anhydride/metal acetylacetonate system is by no means clear at this time. However, research work in this field can go back to as early as 1981 or even earlier [7]. Based on the studies on the bisphenol A/anhydride/metal acetylacetonate system, Smith, *et al.* thought that the decomposition fragments of metal acetylacetonate is the most likely active species responsible for the initiation of polymerization in epoxy/anhydride resins. And they further pointed that the more likely initiation mechanism is the one involving an electron transfer between carboxylic anhydride and the liberated metallic cations to give a reactive initiating species, which can be described in (I) and (II) in Fig. 22 [7]. But this initiation mechanism can not explain the experimental results that both Co^{2+} and Co^{3+} acetylacetonates show virtually the same catalytic reactivity, and the red characteristic color of Co^{2+} generally changes into green characteristic color of Co^{3+} after curing. Therefore, we propose an alternative initiation mechanism here to explain all the experimental results that we had obtained. The initiation mechanism can be schematically shown in (III) and (IV) in Fig. 22. The acetylacetonate anion is gradually released from the metal complex when it is heated to its melting temperature. The enolate type acetylacetonate anion is quite reactive and can effectively attack the carboxylic carbons of the anhydride and form a carboxylic anion which can further open the epoxy ring or another anhydride molecule to initiate anionic polymerization and form crosslinked network. This anionic polymerization is a facile reaction that cures the epoxy underfill in seconds prior to their exit from the surface mount reflow oven.

IV. Conclusion

Metal acetylacetonate is a potent latent catalyst for epoxy/anhydride based no-flow underfill formulations. The curing reaction peak temperature can be manipulated within the range from 195 to 230 °C at the heating rate of 5 °C/min., which is very useful for designing no-flow underfills for solder bump interconnects. The concentration of catalyst mainly affects the curing peak reaction temperature and the weight loss of the underfill during curing, but has little effect on TCE, T_g^{DSC}, T_g^{TMA}, T_g^{DMA}, and crosslinking density of the cured formulations. The concentration of hardener does not noticeably affect the curing profile of the formulations, but do affect the TCE, T_g^{DSC}, T_g^{TMA}, T_g^{DMA}, crosslinking density of the cured formulations, and weight loss of the underfill during curing. Increasing the concentration of hardener results in decreasing of TCE and

increasing of T_g^{TMA} and crosslinking density of the cured samples. The effect of hardener concentration on the T_g^{DSC} and T_g^{DMA} of the cured samples and the weight loss of the underfill during curing depends on the concentration itself. In the low hardener concentration region, increasing the hardener concentration can increase the T_g^{DSC} and T_g^{DMA}, whereas in the high hardener concentration region, increasing hardener concentration results in the decrease of T_g^{DSC} and T_g^{DMA}. The hardener level effect on the weight loss of the underfill during curing depends on the catalyst level. At a low catalyst level, higher hardener concentration results in more weight loss, whereas this effect disappears at high catalyst level. The curing reaction is most likely initiated by the enolate type acetylacetonate anion which is released from the metal acetylacetonate during the no-flow underfill curing.

REFERENCES

[1] C. P. Wong (Ed.), *Polymers for Electronic and Photonic Applications*. New York: Academic, 1993.

[2] R. R. Tummala, E. J. Rymaszewski, and A. Klopfenstein, Eds., *Microelectronics Packaging Handbook*. London, U.K.: Chapman & Hall, 1997.

[3] J. H. Lau, Ed., *Chip on Board*. New York: Van Nostrand Reinhold, 1994.

[4] C. P. Wong and D. F. Baldwin, "No flow underfill for flip-chip packages," U.S. Patent Disclosure, Apr. 1996.

[5] D. R. Gamota and C. M. Melton, "The development of reflowable materials systems to integrate the reflow and underfill dispensing processes for DCA/FCOB assembly," *IEEE Trans. Comp., Packag., Manufact. Technol.*, vol. 20, p. 183, July 1997.

[6] R. W. Pennisi and M. V. Papageorge, "Adhesive and encapsulant material with fluxing properties," U.S. Patent 5 128 746, July 1992.

[7] J. D. B. Smith, "Metal acetylacetonates as latent accelerators for anhydride-cured epoxy resins," *J. Appl. Polym. Sci.*, vol. 26, pp. 979–986, 1981.

[8] AMTECH Technical Bulletin on *Advanced SMT Solder Creams*, 1996.

[9] A. V. Tobolsky, in *Properties and Structure of Polymers*. New York: Wiley, 1960.

[10] C. P. Wong and S. H. Shi, "Low-cost high-performance no-flow underfills for flip-chip applications," U.S. Patent Pending.

[11] C. P. Wong, S. H. Shi, and G. Jefferson, "High performance no-flow underfills for low-cost flip-chip applications," in *Proc. 47th ECTC*, San Jose, CA, May 18–21, 1997, pp. 850–858.

C. P. Wong (SM'87–F'92) received the B.S. degree in chemistry from Purdue University, West Lafayette, IN, and the Ph.D. degree in inorganic/organic chemistry from the Pennsylvania State University, University Park.

After his doctoral study, he was awarded a two-year postdoctoral fellowship with Nobel Laureate Professor Henry Taube at Stanford University, Stanford, CA. He spent 19 years at AT&T Bell Labs. Since 1996, he has been a Professor at the School of Materials Science and Engineering and a Research Director at the NSF Packaging Research Center, Georgia Institute of Technology, Atlanta. His research interests lie in the fields of polymeric materials, high Tc ceramics, materials reaction mechanism, IC encapsulation, in particular, hermetic equivalent plastic packaging, electronic manufacturing packaging processes, interfacial adhesions, PWB, SMT assembly, and components reliability. He is one of the pioneers who demonstrated the use of silicone gel as device encapsulant to achieve reliability without hermeticity in plastic IC packaging. He holds over 40 U.S. patents, numerous international patents, has published over 130 technical papers and 120 key notes and presentations in the related area.

Dr. Wong's awards include the AT&T Bell Laboratories Fellow Award in 1992, the IEEE Components, Packaging, and Manufacturing Technology (CPMT) Society's Outstanding and Best Paper Awards in 1990, 1991, 1994, 1996, and 1998, the IEEE CPMT Society Board of Governors Distinguished Contributions Award in 1991, the IEEE Technical Activities Board (TAB) Distinguished Service Award in 1994, and the 1995 IEEE CPMT Society's Outstanding Sustained Technical Contributions Award (the highest society honor). He is a Fellow of AT&T Bell Labs, and was the General Chairmen of the 41st Electronic Components and Technology Conference in 1991. He served as the Technical Vice President in 1990 and 1991, and the President of the IEEE CPMT Society in 1992 and 1993. He currently chairs the IEEE Technical Activities Board, Steering Committee on Design, and Manufacturing Engineering.

Songhua H. Shi received the B.S. degree from Tsinghua University, Beijing, China, in 1991, the M.S. degree from Fudan University, Shanghai, China in 1994, and is currently pursuing the Ph.D. degree in the School of Materials Science and Engineering, Georgia Institute of Technology, Atlanta.

He was elected a National Science Foundation Fellow of The Packaging Research Center, Georgia Institute of Technology, in 1997.

G. Jeffersen, photograph and biography not available at the time of publication.